Influence of Buffer Species on the Thermodynamics of Short DNA Duplex Melting: Sodium Phosphate versus Sodium Cacodylate†

Saba Alemayehu,‡ Daniel J. Fish,‡ Greg P. Brewood,‡ M. Todd Horne,*,‡ Fidelis Manyanga,‡,§ Rebekah Dickman,‡,§ Ian Yates,‡,§ and Albert S. Benight‡,§

Portland Bioscience Inc., 2828 SW Corbett Ave., Suite 116, Portland, Oregon 97201, and Portland State University, Department of Chemistry, P.O. Box 751, Portland, Oregon 97207

Received: October 21, 2008; Revised Manuscript Received: December 18, 2008

Thermodynamic parameters of the melting transitions of 53 short duplex DNAs were experimentally evaluated by differential scanning calorimetry melting curve analysis. Solvents for the DNA solutions contained ~1 M Na^+ and either 10 mM cacodylate or phosphate buffer. Thermodynamic parameters obtained in the two solvent environments were compared and quantitatively assessed. Thermodynamic stabilities ($\Delta G°$ (25 °C)) of the duplexes studied ranged from quite stable perfect match duplexes (~ −30 kcal/mol) to relatively unstable mismatch duplexes (~ −9 kcal/mol) and ranged in length from 18 to 22 basepairs. A significant difference in stability (average free energy difference of ~3 kcal/mol) was found for all duplexes melted in phosphate (greater stability) versus cacodylate buffers. Measured effects of buffer species appear to be relatively unaffected by duplex length or sequence content. The popular sets of published nearest-neighbor (n-n) stability parameters for Watson−Crick (w/c) and single-base mismatches were evaluated from melting studies performed in cacodylate buffer (SantaLucia and Hicks, *Annu. Rev. Biophys. Biomol. Struct.* **2004**, *33*, 415). Thus, when using these parameters to make predictions of sequence dependent stability of DNA oligomers in buffers other than cacodylate (e.g., phosphate) one should be mindful that in addition to sodium ion concentration, the type of buffer species also provides a minor but significant contribution to duplex stability. Such considerations could potentially influence results of sequence dependent analysis using published n-n parameters and impact results of thermodynamic calculations. Such calculations and analyses are typically employed in the design and interpretation of DNA multiplex hybridization experiments.

Introduction

The most predominant and determinant component of solvents used for DNA melting curve measurements is the monovalent cation (sodium ion) concentration, [Na^+]. In addition to sodium chloride, sodium phosphate, sodium cacodylate, and sodium citrate are commonly used melting solvents that possess desirable buffering properties, such as maximum water solubility, pK_a near 7, and small or negligible temperature dependence of the pK_a over the entire temperature range from 15 to 100 °C where melting experiments are typically performed.[1−7]

During the course of a melting experiment, changes in pK_a with temperature are typically minor, provided the enthalpy of ionization (ΔH_{ion}) and heat capacity changes for buffer ionization are small, and the pH is kept relatively constant. Standard weak base biological buffers (e.g., tris, imidazole) have large ionization enthalpies that compromise their utility in melting experiments. Alternatively, weak acid buffers tend to have small ionization enthalpies and relatively small temperature corrections. The temperature dependence of the pK_a for a number of buffers has been published.[8,9] Reasonably well-behaved buffers meeting the requisite criteria for use in DNA melting experiments are sodium cacodylate ($NaAs(CH_3)_2O_2$), sodium phosphate (Na_3PO_4) and sodium citrate ($Na_3C_6H_5O_7$). Sodium phosphate and cacodylate buffers have been used in a variety of published melting studies and are the buffers compared here.[1−7]

TABLE 1: Recipes for Sodium Phosphate and Sodium Cacodylate Buffers

buffer type	total ion concentration	anion	NaCl	EDTA
sodium phosphate	1000.1 mM Na^+	10 mM Na phosphate	990 mM	0.1 mM
sodium cacodylate	1010.5 mM Na^+	10 mM Na cacodylate	1 M	0.5 mM

Historically, the belief has been that solvent compounds used in melting buffers do not significantly influence DNA duplex stability, other than their effect on the total ionic strength of the solvent. However, this belief has not been rigorously tested and experimental validation is lacking. Here, for the first time results of quantitative experimental evaluation of the effect of buffer species on the thermodynamic properties of DNA hybridization are presented. Over 50 DNA duplexes of varying stabilities in both sodium phosphate and sodium cacodylate buffers were melted by differential scanning calorimetry (DSC). Evaluated thermodynamic parameters in each buffer environment were statistically compared and revealed significant differences.

DNA probe and primer design algorithms employ the nearest-neighbor (n-n) model and associated thermodynamic doublet parameters to generate thermodynamic values for melting nucleic acid duplexes.[3] Recently, the system-wide complexities

† Part of the "J. Michael Schurr Special Section".

* To whom correspondence should be addressed. E-mail: horne@pdxbio.com. Phone: 503-725-2350. Fax: 503-725-2305.

‡ Portland Bioscience Inc.

§ Portland State University.

10.1021/jp809310w CCC: $40.75
Published on Web 02/09/2009

TABLE 2: Sequences of the 53 duplexes studied in DSC melting experiments[a]

ID	sequence (5′→3′)	ID	sequence (5′→3′)
PM-1	TGCGATCGCACTTAGCGA	2 × 2-1	GCATAAGC**A**ga**A**GGATAGTC
PM-2	TGCGGTAGCGATTGGGCGC	2 × 2-2	------**A**ga**T**------
PM-3	TGCGAGCCGTTGATAGCGG	2 × 2-3	------**A**ga**G**------
PM-4	AGCGCGCCATAGAAGTGCGA	2 × 2-4	------**A**ga**C**------
PM-5	AGCGAACTGGCGATTAGCGC	2 × 2-5	------**T**ga**A**------
PM-6	AGCGATAACTCGCCCAGGCGG	2 × 2-6	------**T**ga**T**------
PM-7	CGCGATGCTTCCGTTATGCGC	2 × 2-7	------**T**ga**G**------
PM-8	CGCGATGAACCGCTGTAGGCGG	2 × 2-8	------**T**ga**C**------
PM-9	GGCGAACTGGCGATATTAGCGG	2 × 2-9	------**G**ga**A**------
PM-10	TATACGAACTATGGATAT	2 × 2-10	------**G**ga**T**------
PM-11	TATATTCATAGCGTATAA	2 × 2-11	------**G**ga**G**------
PM-12	TATACTGCGTATTCCATAC	2 × 2-12	------**G**ga**C**------
PM-13	TATATCATAAGCGGTATAG	2 × 2-13	------**C**ga**A**------
PM-14	AATAGCCTTATCACCGATAA	2 × 2-14	------**C**ga**T**------
PM-15	AATATGCGGACTAAATATAC	2 × 2-15	------**C**ga**G**------
PM-16	AATACATTACTCGGCGCATAG	2 × 2-16	------**C**ga**C**------
PM-17	CATAATAACTCCGCTGTATAC	4 × 4-1	CATAAGC**A**ggaa**A**GGATAGC
PM-18	CATAATAGCCGTTGTCGGATAG	4 × 4-2	------**A**gaga**A**------
PM-19	GATAGCCGTTATCAGTAAATAG	4 × 4-3	------**A**gcta**A**------
2 × 2 p.m.-1	GACTATCCCTCTGCTTATGC	4 × 4-4	------**A**gtca**A**------
2 × 2 p.m.-2	GCATAAGCATCGGGATAGTC	4 × 4-5	------**G**ggaa**G**------
2 × 2 p.m.-3	GACTATCCTTCCGCTTATGC	4 × 4-6	------**G**gaga**G**------
2 × 2 p.m.-4	GCATAAGCGTCAGGATAGTC	4 × 4-7	------**G**gcta**G**------
2 × 2 p.m.-5	GACTATCCCTCCGCTTATGC	4 × 4-8	------**G**gtca**G**------
2 × 2 p.m.-6	GCATAAGCGTCGGGATAGTC	4 × 4-9	------**A**cgat**A**------
2 × 2 p.m.-7	GACTATCCGTCGGCTTATGC	4 × 4-10	------**A**cagt**A**------
2 × 2 p.m.-8	GCATAAGCCTCCGGATAGTC		

[a] Uppercase letters indicate w/c base pairs. Lower case letters indicate mismatch base-pairs where a is paired with g and c with t. Bold upper case letters highlight the different w/c base pairs surrounding the mismatched bases. For both 2 × 2 and 4 × 4 mismatched duplexes, the sequences flanking the central mismatched region remained unchanged, indicated by dashed lines.

inherent to DNA multiplex reactions were described, and a generalized theory for predicting kinetic and equilibrium binding propensities based on such calculated thermodynamic parameters was presented.[10] The intent of that work was to provide a comprehensive and platform independent format to enable accurate prediction of hybridization reactions. Of course, quality of the predictions depends on accuracy of the thermodynamic parameters used as input. Current microarray hybridization approaches typically have more than 10^6 probes attached to a small surface on which multiplex hybridization with multiple targets occurs. Optimum design of such multiplex hybridization reactions requires detailed knowledge of the relative sequence dependent stability of all potential probe/target complexes and how they will behave in such a complex environment. Such reactions form the basis of nucleic acid diagnostic tests. Thus, results of this study can be used to improve predictive accuracy of diagnostic DNA hybridization reactions.

Experimental Methods

Melting Buffers. Compositions of phosphate and cacodylate buffer solutions were taken from the literature and prepared as described.[1,11] Both sodium phosphate and sodium cacodylate buffers were prepared according to recipes shown in Table 1. HCl was used to adjust solution acidity of both buffers to 7.4 < pH < 7.8. The phosphate buffer with pK_a = 7.20 buffers well over the pH range from 5.8 to 8.0.[11] The 1.0 M 3·Na^+/PO_4^{3-} melting buffer was prepared as a solution containing a mixture of 990 mM NaCl (Fluka), 10 mM sodium phosphate (Sigma) and 0.1 mM EDTA (Sigma). Ethylendiaminetetraacetic acid (EDTA) was added to remove trace amounts of divalent and trivalent ions that bind to DNA potentially compromising results obtained from the melting process.[12] The pH of the buffered phosphate solution was 7.4. The cacodylate buffer, with pK_a = 6.27, buffers well over the pH range 5.0−7.4. As reported,[1] the Na^+-cacodylate buffer was prepared as a solution of 1.0 M NaCl (Fluka), 10 mM sodium cacodylate ($(CH_3)_2AsO_2Na·3H_2O$) (Fisher) and 0.5 mM EDTA (Sigma).

Differential Scanning Calorimetry (DSC). Thermodynamic parameters of DNA hybridization are routinely evaluated using two standard techniques: (1) UV optical absorbance measurements around 260 nm as a function of temperature and (2) DSC, which provides a direct measurement of the excess heat capacity, ΔC_p, versus temperature. Analyses of ΔC_p versus temperature curves using DSC provide a direct evaluation of the melting thermodynamics. Evaluation of thermodynamic parameters from UV-absorbance melting curves inherently requires that the transition occurs in a two-state manner. For this reason, UV spectroscopy probably lacks sensitivity sufficient to detect subtle influences of the melting buffer. Conversely, DSC provides a direct measurement of the melting thermodynamics without invoking a model of the transition.

Thermodynamic parameters, $\Delta H°$, $\Delta S°$, and $\Delta G°$ for melting short DNA duplexes were evaluated from DSC melting curves. Throughout this study, we have assumed that the overall heat capacity change, $\Delta\Delta C_p = \Delta C_p(\text{final}) - \Delta C_p(\text{initial})$, of the melting transition in each buffer is negligible. In the few cases that have attempted to evaluate the net heat capacity difference for DNA melting, the derived value has been found to be relatively small, but nonzero.[13−16] This is clearly an issue yet to be settled. We assume $\Delta\Delta C_p = 0$ for if this were not the case, contrary to what was observed (see Results below), the relative ordering of $\Delta G°$ values measured in different buffers would not be expected to be preserved for all the DNAs.

Melting curves of the excess heat capacity ΔC_p of DNA solutions versus temperature were obtained using a Nano-DSC (Calorimetry Sciences Corp.) and a heating rate of 75 °C/hour (from

TABLE 3: Thermodynamic Parameters Evaluated Using DSC in Both Cacodylate and Phosphate Buffers: (a) 4 × 4 Tandem Mismatches in the Center; (b) 2 × 2 Tandem Mismatches in the Center; (c) Perfect Match Duplexes of Varying Lengths

			cacodylate buffer								phosphate buffer							
ID	length	%GC	ΔH kcal/mol	σ^2	ΔS e.u.	σ^2	T_m °C	σ^2	ΔG_{25} kcal/mol	σ^2	ΔH kcal/mol	σ^2	ΔS e.u.	σ^2	T_m °C	σ^2	ΔG_{25} kcal /mol	σ^2
(a)																		
4 × 4−1	20	45	−113.5	3.8	−337.0	10.4	63.0	0.2	−13.0	0.8	−137.2	2.3	−407.0	6.8	64.0	0.1	−15.9	0.3
4 × 4−2	20	45	−123.7	2.5	−366.3	7.1	64.2	0.3	−14.5	0.4	−132.8	1.7	−393.0	4.9	64.7	0.1	−15.7	0.3
4 × 4−3	20	45	−91.3	2.2	−274.8	6.5	58.9	0.3	−9.4	0.2	−103.5	0.8	−311.3	2.6	59.3	0.1	−10.8	0.1
4 × 4−4	20	45	−123.3	1.4	−371.3	4.3	58.8	0.0	−12.6	0.2	−142.4	0.9	−427.5	3.1	59.8	0.1	−15.0	0.1
4 × 4−5	20	55	−127.7	0.9	−372.5	2.9	69.8	0.4	−16.7	0.1	−146.7	1.2	−427.0	3.7	70.3	0.1	−19.4	0.1
4 × 4−6	20	55	−147.9	2.3	−430.0	7.1	70.8	0.1	−19.7	0.2	−168.2	2.2	−437.8	6.4	71.9	0.1	−22.8	0.3
4 × 4−7	20	55	−1057	2.1	−313.3	5.9	64.2	0.3	−12.3	0.3	−125.5	1.8	−371.0	5.5	65.0	0.1	−14.9	0.2
4 × 4−8	20	55	−123.8	1.0	−366.0	2.9	65.1	0.1	−14.7	0.1	−136.5	1.5	−402.5	4.7	65.8	0.2	−16.6	0.1
4 × 4−9	20	45	−95.6	2.9	−289.5	8.7	57.0	0.2	−9.3	0.3	−108.3	2.1	−327.0	6.5	57.7	0.1	−10.8	0.2
4 × 4−10	20	45	−107.3	1.7	−322.8	5.0	59.3	0.1	−11.1	0.2	−124.1	1.4	−372.8	3.9	59.7	0.2	−13.0	0.2
(b)																		
2 × 2−1	20	45	−108.5	1.8	−316.8	5.4	69.3	0.1	−14.1	0.2	−131.8	2.6	−383.8	7.6	70.4	0.1	−17.4	0.3
2 × 2−2	20	45	−125.4	1.5	−364.5	4.1	70.9	0.1	−16.8	0.3	−132.6	2.2	−385.0	6.7	71.1	0.0	−17.8	0.3
2 × 2−3	20	50	−99.5	0.8	−288.0	2.4	71.7	0.7	−13.7	0.1	−116.6	0.4	−337.0	0.8	72.8	0.1	−16.2	0.2
2 × 2−4	20	50	131.4	1.3	−378.3	3.4	74.2	0.1	−18.7	0.3	−147.1	2.3	−423.5	6.5	74.1	0.1	−20.8	0.4
2 × 2−5	20	45	126.2	1.9	−364.8	6.1	72.7	0.3	−17.5	0.1	−136.9	2.4	−395.8	6.3	72.9	0.3	−19.0	0.5
2 × 2−6	20	45	−125.7	2.2	−366.5	5.8	69.9	0.4	−18.5	0.5	−151.6	1.3	−441.0	3.8	70.5	0.1	−20.2	0.2
2 × 2−7	20	50	−97.7	3.9	−280.5	11.0	75.5	0.2	−14.1	0.6	−117.7	0.8	−338.0	0.8	75.8	0.1	−17.0	0.6
2 × 2−8	20	50	−108.6	1.2	−312.8	3.8	74.3	0.4	−15.4	0.1	−142.0	2.0	−408.5	5.7	74.2	0.1	−20.2	0.3
2 × 2−9	20	50	−124.2	1.6	−358.3	4.9	73.5	0.1	−17.5	0.1	−134.1	2.0	−387.0	5.4	73.6	0.1	−18.8	0.4
2 × 2−10	20	50	−108.1	0.1	−311.3	0.5	74.1	0.1	−15.4	0.1	−127.1	1.3	−385.0	3.5	74.8	0.3	−18.3	0.3
2 × 2−11	20	55	−106.2	1.4	−304.5	4.2	75.6	0.0	−15.4	0.1	−123.8	3.0	353.0	8.4	77.6	0.1	−18.6	0.5
2 × 2−12	20	55	−110.7	1.0	−316.5	3.5	76.5	0.1	−16.4	0.2	−127.5	1.9	−365.3	5.5	75.6	0.1	−18.6	0.2
2 × 2−13	20	50	−145.5	0.0	−417.8	2.1	75.1	0.0	−21.0	0.1	−158.5	3.1	−454.8	9.0	75.7	0.1	−23.0	0.4
2 × 2−14	20	53	−129.7	0.7	−374.0	1.6	73.8	0.5	−18.2	0.3	−137.6	1.7	−396.0	5.2	74.0	0.1	−19.5	0.3
2 × 2−15	20	55	−106.7	1.7	−304.0	4.9	77.9	0.2	−16.1	0.3	−119.1	2.1	−338.8	5.6	78.4	0.3	−18.2	0.5
2 × 2−16	20	55	−102.9	3.4	−293.5	9.3	77.4	0.4	−15.4	0.4	−111.7	2.1	−318.3	6.1	77.6	0.0	−16.9	0.3
(c)																		
PM-1	18	55.6	−76.0	4.7	−214.8	13.1	90.9	0.3	−12.0	0.8	−111.9	2.9	−315.3	8.2	82.1	0.0	−18.0	0.5
PM-2	19	68.4	−105.9	3.3	−295.0	9.1	85.9	0.2	−18.0	0.6	−126.2	1.1	−351.0	2.9	86.1	0.0	−21.6	0.3
PM-3	20	63.2	−87.7	2.3	−245.0	8.5	84.5	0.1	−14.7	0.4	−123.5	2.7	−343.8	7.2	86.0	0.2	−21.1	0.6
PM-4	20	60.0	−48.4	3.5	−135.8	9.9	83.6	0.3	−7.9	0.5	−77.9	4.4	−218.0	12.3	84.1	0.2	−12.9	0.8
PM-5	20	60.0	−33.5	1.3	−233.8	3.6	83.8	0.1	−13.8	0.2	−139.1	1.4	−388.0	3.8	85.1	0.1	−23.4	0.3
PM-6	21	66.7	−127.8	2.2	−355.5	8.6	86.4	0.2	−21.8	0.3	−160.9	1.5	−447.0	4.1	89.9	0.2	−27.7	0.3
PM-7	21	61.9	−123.8	2.1	−360.0	5.7	84.3	0.3	−21.5	0.4	−151.6	3.2	−424.3	9.4	34.7	0.1	−25.2	0.5
PM-8	22	69.2	−158.0	2.9	−439.5	8.4	86.6	0.0	−27.0	0.4	−186.4	2.9	−518.0	8.0	86.7	0.2	−32.0	0.5
PM-9	22	59.1	−148.5	3.7	−414.5	10.4	84.7	0.1	−24.9	0.6	−187.7	1.2	−524.0	3.9	84.9	0.4	−31.5	0.1
PM-10	18	27.8	−97.0	1.2	−282.8	3.3	69.7	0.1	−12.7	0.2	−118.9	2.4	−345.8	7.1	70.6	0.1	−15.8	0.3
PM-11	18	22.2	−56.0	4.5	−164.8	13.2	66.6	0.1	−6.9	0.6	−86.5	1.3	−254.8	3.5	66.6	0.1	−10.6	0.2
PM-12	19	36.8	−88.9	5.4	−257.0	15.9	73.1	0.0	−12.3	0.7	−116.1	3.4	−335.3	9.7	73.7	0.1	−16.2	0.5
PM-13	19	31.6	−108.8	2.5	−315.8	7.2	71.6	0.1	−14.7	0.4	−119.9	2.4	−348.0	7.0	71.1	0.1	−16.1	0.4
PM-14	20	35.0	−105.7	0.6	−302.8	1.7	76.1	0.1	−15.5	0.2	−129.6	4.7	−370.8	13.5	76.7	0.1	−19.1	0.7
PM-15	20	30.0	−121.3	1.0	−350.3	3.1	73.0	0.1	−16.9	0.1	−137.7	1.5	−396.8	4.3	73.8	0.2	−19.5	0.2
PM-16	21	42.9	−131.7	2.9	−372.3	8.3	80.8	0.2	−20.8	0.4	−153.7	1.6	−434.8	4.3	80.6	0.2	−24.1	0.3
PM-17	21	38.1	−133.0	3.8	−383.0	11.4	74.1	0.2	−18.9	0.5	−156.2	4.4	−449.0	12.8	74.5	0.2	−22.3	0.6
PM-18	22	45.5	−139.4	3.0	−394.8	8.5	80.0	0.1	−21.7	0.5	−166.0	2.7	−470.0	7.5	79.9	0.3	−25.9	0.5
PM-19	22	36.4	−144.1	2.1	−413.5	6.2	75.4	0.0	−20.9	0.2	−164.0	3.2	−470.5	9.3	75.4	0.1	−23.7	0.5
PM-2 × 2−1	20	50.0	−148.6	1.3	−424 3	3.3	77.1	0.1	−22.2	0.3	−162.3	3.7	−463.5	10.3	76.9	0.2	−24.2	0.6
PM-2 × 2−2	20	50.0	−154.0	2.9	−438.5	8.2	78.2	0.3	−23.4	0.5	−166.1	1.9	−472.5	4.7	78.3	0.3	−25.3	0.5
PM-2 × 2−3	20	50.0	−156.1	1.3	−445.3	3.8	77.4	0.2	−23.4	0.2	−165.0	4.9	−470.5	13.5	77.5	0.2	−24.8	0.8
PM-2 × 2−4	20	45.0	−149.3	2.3	−424.8	6.4	77.8	0.4	−22.7	0.4	−152.8	4.9	−435.0	13.9	78.0	0.2	−23.1	0.8
PM-2 × 2−5	20	55.0	−149.1	2.2	−424.0	6.2	78.4	0.1	−22.7	0.4	−164.2	3.4	−466.3	9.0	79.0	0.1	−25.2	0.7
PM-2 × 2−6	20	55.0	−135.6	3.2	−384.3	6.0	80.1	0.3	−21.1	0.6	−154.8	2.1	−437.8	6.0	80.6	0.4	−24.4	0.4
PM-2 × 2−7	20	55.0	−144.3	2.3	−408.3	6.5	80.1	0.1	−22.6	0.4	−181.7	0.9	−457.3	2.6	80.4	0.1	−25.4	0.1
PM-2 × 2−6	20	55.0	−145.6	2.9	−413.0	7.6	79.3	0.3	−22.6	0.6	−161.5	0.9	−457.8	2.8	79.6	0.3	−25.1	0.2

15 to 90 °C). The average buffer baseline determined from multiple (more than eight) scans of each buffer versus buffer alone was subtracted from the sample melting curve recorded in that buffer. This process minimized effects that might be associated with differences in buffer heat capacities and ensured that behaviors of the buffer alone did not manifest in melting curves unless they were directly associated with the DNA.

A quadratic polynomial baseline was fit to the curve and the resulting baseline-corrected curve was normalized to the total DNA concentration to obtain the DSC melting curve. Thermodynamic transition parameters $\Delta H°$ and $\Delta S°$ were determined from the normalized, baseline-corrected, ΔC_p versus T curve via integration.[17,18] Analysis to obtain the calorimetric transition enthalpy ($\Delta H°$) and entropy ($\Delta S°$) was performed using the

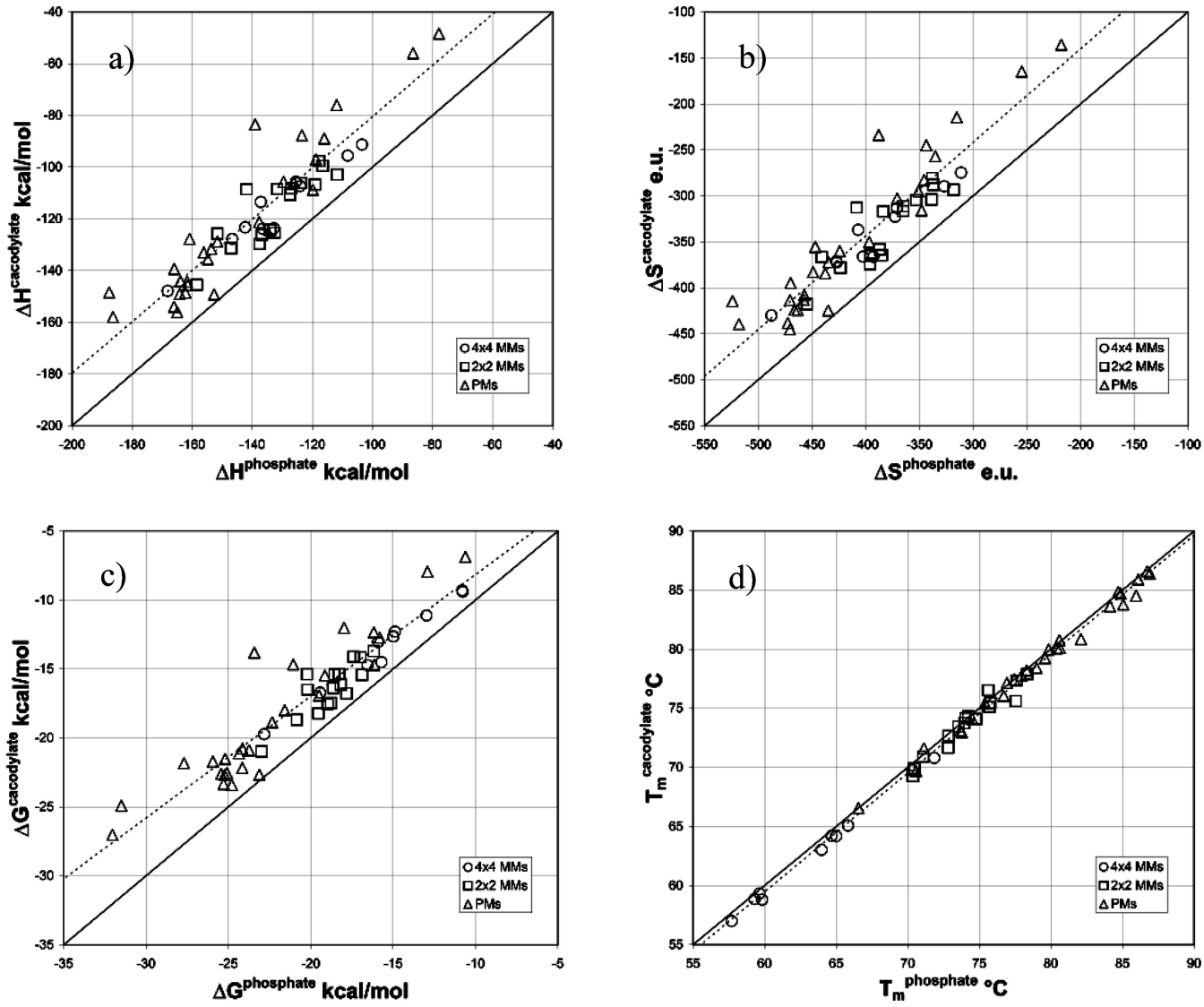

Figure 1. Scatter plots of thermodynamic values evaluated in the cacodylate buffer versus those evaluated in the phosphate buffer. The dashed lines are the linear fits for all duplexes, the line $y = x$ is shown as a solid black line for reference. Relevant statistical values associated with these linear fits are summarized in Table 4 and the equations of the linear fits follow. (a) $\Delta H^{\text{cacodylate}} = 0.9927 \cdot \Delta H^{\text{phosphate}} + 18.845$, $R^2 = 0.8512$; (b) $\Delta S^{\text{cacodylate}} = 1.0191 \cdot \Delta S^{\text{phosphate}} + 64.11$, $R^2 = 0.8546$; (c) $\Delta G^{\text{cacodylate}} = 0.8829 \cdot \Delta G^{\text{phosphate}} + 0.6812$, $R^2 = 0.8808$; (d) $T_m^{\text{cacodylate}} = 1.0069 \cdot T_m^{\text{phosphate}} - 0.9596$, $R^2 = 0.9954$.

Cpcalc routine (Calorimetry Sciences Corp.). Free energy, $\Delta G°$, was determined as $\Delta G° = \Delta H° - T\Delta S°$ with $T = 298.15$ K. Routinely, at least three forward (heating) and reverse (cooling) ΔC_p versus T scans were made per melting experiment. DNA concentration for each DNA duplex was determined from the specific molar extinction coefficient of the sequence, and DNA absorbance readings at 260 nm. For all DSC melting experiments DNA concentrations ranged from 75−130 μM.

DNA Sequences. Sequences of the 53 short duplex DNAs employed in this study are given in Table 2. The set of duplex DNAs is composed of 27 perfect match duplexes and 26 duplexes containing different combinations of 5′-GA-3′/3′-AG-5′ and 5′-AG-3′/3′-GA-5′ tandem mismatches. The G + C content of the duplexes ranged from 22 to 68% with a median of 45%. Duplex length varied from 18 to 22 base pairs.

Four types of DNA duplexes were studied. (1) 10 20-mer duplexes containing 4 × 4 tandem mismatches (labeled 4 × 4-*N*, $N = 1-10$); (2) 16 20-mer duplexes containing 2 × 2 tandem mismatches (labeled 2 × 2-*N*, $N = 1-16$); (3) 8 perfect match 20-mer duplexes (labeled PM-2 × 2-*N*, $N = 1-8$) that complement a subset of the 2 × 2 mismatched duplexes; and (4) 19 additional perfect match duplexes (labeled PM-*N*, $N = 1-19$) with lengths varying from 18 to 22 base-pairs.

Synthetically prepared and purified single strands used to make the short oligoduplexes were synthesized on a one micromole scale and purchased from Integrated DNA Technologies (IDT). Average yield for each sample was 25−30 OD/ml. After suspension in the buffer solutions, DNA concentrations were determined from absorbance readings at 260 nm using Beer's Law and known molar extinction coefficients of the DNA strands.

Results

Melting Experiments. Thermodynamic parameters of the melting transitions for the 53 DNA duplexes shown in Table 2 were measured by DSC in both cacodylate and phosphate buffer environments. Results of over 100 DSC melting curves measured for these molecules are summarized in Table 3. Variances shown in Table 3 were determined from multiple experiments and experimental reproducibility. Thermodynamic parameters, $\Delta H°$, $\Delta S°$, $\Delta G°$ and transition temperatures, T_m, evaluated from

TABLE 4: Statistics Associated with the Linear Fits of the Cacodylate versus Phosphate Plots Shown in Figure 1[a]

	ΔH kcal/mol						
	R^2	m	se_m	b	se_b	se_y	FDIST
4 × 4 MM's	0.95	0.87	0.07	−0.36	9.94	4.18	2.5E-06
2 × 2 MM's	0.74	0.89	0.14	2.00	18.86	7.24	2.0E-05
PM's	0.89	1.08	0.08	35.33	11.43	10.82	2.8E-13
ALL	0.85	0.99	0.06	1885	8.16	9.56	9.6E-23
	ΔS e.u.						
	R^2	m	se_m	b	se_b	se_y	FDIST
4 × 4 MM's	0.94	0.87	0.08	−1.81	31.97	12.40	4.8E-06
2 × 2 MM's	0.75	0.89	0.14	2.96	52.58	20.80	1.5E-05
PM's	0.89	1.11	0.08	109.00	31.93	29.57	1.3E-13
ALL	0.89	1.11	0.08	109.00	31.93	29.57	1.9E-23
	ΔG_{25} kcal/mol						
	R^2	m	se_m	b	se_b	se_y	FDIST
4 × 4 MM's	0.98	0.87	0.04	0.11	0.71	0.50	5.3E-08
2 × 2 MM's	0.71	0.94	0.16	1.17	3.01	1.06	4.1E-05
PM'S	0.87	0.96	0.08	2.88	1.74	1.96	2.2E-12
ALL	0.88	088	0.05	068	0.93	1.58	3.3E-25
	T_m °C						
	R^2	m	se_m	b	se_b	se_y	FDIST
4 × 4 MM's	1.00	0.98	0.02	0.33	1.15	0.26	1.4E-11
2 × 2 MM's	0.94	1.00	0.07	−0.05	5.13	0.65	8.7E-10
PM'S	0.99	0.98	0.02	1.29	1.36	0.47	4.8E-28
ALL	1.00	1.01	0.01	−0.96	0.72	0.51	3.5E-61

[a] R^2 is the correlation coefficient, m and b are the slopes and intercepts of the linear fits, respectively, and se_m, se_b, and se_y are the standard errors of the slopes, intercepts and y-values respectively. FDIST is the probably of observing the given correlation by chance (see text for a more detailed discussion of the statistical quantities employed).

DSC melting curves in the two buffers are plotted versus each other in scatter plots in Figure 1. Similarities of each set of parameters evaluated in the two buffer environments were quantitatively assessed by linear statistical analysis of the plots. Examples of DSC melting curves for a selection of duplexes can be found in Supporting Information.

Correlations of Data. Results for linear fits of the scatter plots displayed in Figure 1 are summarized in Table 4. Parameters m and b are the best fit slope and intercept of the linear regression fit to the equation, $y = mx + b$. Values of these parameters indicate whether the two sets of thermodynamic values being compared are within the same (in a quantitative statistical sense) range and scale. Standard errors on m, b, and y are specified by the values of se_m, se_b, and se_y, respectively. Values of the correlation coefficient, R^2, approaching 1.0 indicate thermodynamic parameters determined in the two buffer environments are well-correlated, that is, differences in the two sets of values can be resolved by a suitable scaling term. Quality of the agreement is quantified by the parameter FDIST, which represents the probability of finding the given correlation by random chance using the F-test statistic.[19]

Inspection of the results in Table 4 reveals high R^2 values (near 1.0) for nearly all linear fits, indicating that stability ordering is preserved for nearly all thermodynamic parameters. In all cases, DNA duplexes in cacodylate buffer were found to be less stable than the same duplexes in phosphate buffer, even though $[Na^+]$ is slightly higher in the cacodylate buffer (see Table 1). The smallest differences (i.e., smallest intercepts, b) in free energy, are seen for duplexes containing mismatches, with $b = 0.11$ kcal/mol for 4 × 4 mismatches. In general, differences in the values of $\Delta H°$, $\Delta S°$, and $\Delta G°$ for the duplexes containing 4 × 4 mismatches were smaller than for those containing 2 × 2 mismatches. For the measured T_m values, the perfect match duplexes show the largest difference ($b = 1.29$ °C). On average, these differences are greatest for the most stable duplexes; however, no correlation was found between stability of the perfect matches (which have a wide range of stabilities) and amount of the difference. Rather, differences between experimental parameters evaluated for the DNAs in the two buffer environments seem to be a function of the class of duplexes (e.g., 4 × 4 tandem mismatches, 2 × 2 tandem mismatches and perfect matches). On average, perfect match duplexes were destabilized in the cacodylate buffer by 3.7 ± 1.9 kcal/mol compared to phosphate buffer, regardless of relative stability or length of the DNA duplexes.

These results suggest the average geometry of the duplex may be a contributing factor in the observed relative differences in stability for perfect match and mismatch duplexes in phosphate versus cacodylate melting buffers. Differences are greatest for perfect match duplexes, and least for 4 × 4 tandem mismatch duplexes, with 2 × 2 tandem mismatch duplexes falling in between. Sequences of the 2 × 2 tandem mismatch duplexes of this study all contain a GA/AG tandem mismatch. Although notorious for being an exceptionally stable tandem mismatch, and well tolerated within the geometry of a w/c (Watson−Crick) B-form duplex, this tandem mismatch is also known to induce significant perturbations in the local twist of the B-form DNA duplex.[20−25] More drastic structural perturbations of the duplex geometry are induced by the 4 × 4 tandem mismatches that results in smaller differences between experimental parameters evaluated in the two buffer environments. Collected data supports the notion that observed differences in thermodynamic parameters evaluated in cacodylate versus phosphate buffers are greater for those duplexes having the least perturbed native structure. Consequently, the greater the perturbation, the lower effects of different buffer environments. Differences in the measured T_m, a common experimental parameter used to compare stabilities of short duplex DNAs, of perfect matches and duplexes containing mismatches (in both buffer environments) are not as large in all cases.

Average Differences. Differences in thermodynamic parameter values determined in cacodylate and phosphate buffers are summarized in Table 5. Entries are sorted from the smallest difference in free energy ($\Delta\Delta G = \Delta G°$(cacodylate) − $\Delta G°$(phosphate), top) to the greatest difference (bottom). Figure 2 shows ΔG_{25} values from Table 3 for each duplex measured in both buffers. The data in Figure 2 is organized from left to right with the smallest difference in ΔG_{25} values on the left to the greatest difference on the right. Likewise, Figure 3 shows the difference in T_m values, T_m(cacodylate) − T_m(phosphate) for each duplex sorted from smallest difference (left) to greatest difference (right). Differences in melting temperatures varied from −2.0 ± 0.1 to 0.9 ± 0.1 °C. Average differences for each class of duplex are shown in Table 6. Perfect match duplexes exhibited an average difference in free energy, $\Delta\Delta G = 3.7 \pm 1.9$ kcal/mol; duplexes having 2 × 2 mismatches gave an average $\Delta\Delta G = 2.4 \pm 1.0$ kcal/mol, while duplexes with 4 × 4 mismatches had an average $\Delta\Delta G = 2.1 \pm 0.7$ kcal/mol. Over all duplex types, an average of $\Delta\Delta G = 3.0 \pm 1.7$ kcal/mol was found. When grouped according to duplex type, PM-N duplexes have the highest difference in free energies ($\Delta\Delta G = 4.4 \pm 1.8$ kcal/mol). This set of molecules contains the longest duplexes having the highest GC%. No significant differences in $\Delta\Delta G$

TABLE 5: Differences between Cacodylate and Phosphate Thermodynamic Parameters, $\Delta\Delta X = X$(Cacodylate) − X(Phosphate), Sorted from Least $\Delta\Delta G$ (Top) to Greatest $\Delta\Delta G$ (Bottom)

ID	sequence	$\Delta\Delta H$ kcal/mol	σ^2	$\Delta\Delta S$ e.u.	σ^2	ΔT_m °C	σ^2	$\Delta\Delta G_{25}$ kcal/mol	σ^2
PM-2 × 2-4	GCATAAGCGTCAGGATAGTC	3.5	5.4	10.3	15.3	−0.2	0.5	0.4	0.9
2 × 2-2	GCATAAGCAgaTGGATAGTC	7.2	2.7	20.5	7.9	−0.2	0.1	1.0	0.4
4 × 4-2	CATAAGCAgagaAGGATAGC	9.2	3.0	26.8	8.7	−0.5	0.4	1.2	0.5
2 × 2-9	GCATAAGCGgaAGGATAGTC	9.9	2.6	28.8	7.3	−0.1	0.1	1.3	0.4
2 × 2-14	GCATAAGCCgaTGGATAGTC	7.9	1.9	22.0	5.5	−0.2	0.5	1.3	0.4
4 × 4-3	CATAAGCAgctaAGGATAGC	12.3	2.3	36.5	7.0	−0.4	0.3	1.4	0.3
PM-2 × 2-3	GACTATCCTTCCGCTTATGC	8.9	5.0	25.3	14.0	0.0	0.3	1.4	0.9
2 × 2-5	GCATAAGCTgaAGGATAGTC	10.7	3.0	31.0	8.7	−0.2	0.4	1.4	0.5
PM-13	TATATCATAAGCGGTATAG	11.1	3.5	32.3	10.0	0.5	0.1	1.4	0.5
2 × 2-16	GCATAAGCCgaCGGATAGTC	8.8	4.0	24.8	11.6	−0.3	0.4	1.4	0.5
4 × 4-9	CATAAGCAcgatAGGATAGC	12.7	3.6	37.5	10.8	−0.7	0.3	1.5	0.4
4 × 4-8	CATAAGCGgtcaGGGATAGC	12.7	1.8	36.5	5.5	−0.8	0.2	1.8	0.2
4 × 4-10	CATAAGCAcagtAGGATAGC	16.8	2.2	50.0	6.4	−0.3	0.2	1.8	0.3
PM-2 × 2-2	GCATAAGCATCGGGATAGTC	12.1	3.4	34.0	9.4	−0.1	0.5	1.9	0.7
PM-2 × 2-1	GACTATCCCTCTGCTTATGC	13.7	3.9	39.3	10.9	0.2	0.2	2.0	0.7
2 × 2-13	GCATAAGCCgaAGGATAGTC	13.0	3.2	37.0	9.3	−0.6	0.1	2.0	0.4
2 × 2-15	GCATAAGCCgaGGGATAGTC	12.4	2.8	34.8	7.4	−0.4	0.4	2.0	0.6
2 × 2-4	GCATAAGCAgaCGGATAGTC	15.7	2.6	45.3	7.3	0.1	0.1	2.2	0.4
2 × 2-12	GCATAAGCGgaCGGATAGTC	16.8	2.1	48.8	6.0	0.9	0.1	2.2	0.3
4 × 4-4	CATAAGCAgtcaAGGATAGC	19.1	1.7	56.3	5.3	−1.0	0.1	2.3	0.2
2 × 2-3	GCATAAGCAgaGGGATAGTC	17.1	0.9	49.0	2.6	−1.2	0.7	2.5	0.2
PM-2 × 2-5	GACTATCCCTCCGCTTATGC	15.1	4.0	42.3	10.9	−0.6	0.1	2.5	0.8
PM-2 × 2-8	GCATAAGCCTCCGGATAGTC	15.9	3.0	44.8	8.1	−0.3	0.5	2.5	0.6
PM-15	AATATGCGGACTAAATATAC	16.4	1.8	46.5	5.3	−0.8	0.2	2.6	0.3
4 × 4-7	CATAAGCGgctaGGGATAGC	19.8	2.8	57.8	8.0	−0.8	0.3	2.6	0.4
4 × 4-5	CATAAGCGggaaGGGATAGC	19.0	1.5	54.5	4.7	−0.5	0.4	2.7	0.2
PM-2 × 2-7	GACTATCCGTCGGCTTATGC	17.4	2.5	49.0	7.0	−0.3	0.2	2.8	0.4
PM-19	GATAGCCGTTATCAGTAAATAG	19.8	3.S	57.0	11.1	0.0	0.1	2.8	0.6
2 × 2-7	GCATAAGCTgaGGGATAGTC	20.0	4.0	57.5	11.1	−0.3	0.2	2.8	0.9
4 × 4-1	CATAAGCAggaaAGGATAGC	23.7	4.5	70.0	12.5	−1.0	0.2	2.9	0.8
2 × 2-10	GCATAAGCGgaTGGATAGTC	18.9	1.3	53.8	3.5	−0.7	0.3	2.9	0.3
PM-10	TATACGAACTATGGATAT	21.9	2.7	63.0	7.8	−0.9	0.2	3.1	0.4
4 × 4-6	CATAAGCGgagaGGGATAGC	20.3	3.2	57.8	9.6	−1.1	0.1	3.1	0.4
2 × 2-11	GCATAAGCGgaGGGATAGTC	17.6	3.3	48.5	9.4	−2.0	0.1	3.1	0.5
PM-2 × 2-6	GCATAAGCGTCGGGATAGTC	19.2	3.9	53.5	10.9	−0.5	0.5	3.2	0.7
2 × 2-1	GCATAAGCAgaAGGATAGTC	23.3	3.1	67.0	9.3	−1.1	0.1	3.3	0.4
PM-16	AATACATTACTCGGCGCATAG	22.0	3.3	62.5	9.4	0.2	0.2	3.4	0.5
PM-17	CATAATAACTCCGCTGTATAC	23.2	5.9	66.0	17.2	−0.4	0.3	3.5	0.8
PM-2	TGCGGTAGCGATTGGGCGC	20.3	3.5	56.0	9.5	−0.2	0.2	3.6	0.7
PM-14	AATAGCCTTATCACCGATAA	23.9	4.8	68.0	13.6	−0.7	0.1	3.7	0.7
2 × 2-6	GCATAAGCTgaTGGATAGTC	25.9	2.6	74.5	7.0	−0.5	0.4	3.7	0.6
PM-7	CGCGATGCTTCCGTTATGCGC	22.8	3.8	64.3	11.0	0.1	0.4	3.7	0.6
PM-11	TATATTCATAGCGTATAA	30.6	4.7	90.0	13.7	0.0	0.1	3.7	0.6
PM-12	TATACTGCGTATTCCATAC	27.2	6.4	78.3	18.6	−0.6	0.1	3.8	0.9
PM-18	CATAATAGCCGTTGTCGGATAG	26.7	4.1	75.3	11.4	0.1	0.3	4.2	0.7
2 × 2-8	GCATAAGCTgaGGGATAGTC	33.4	2.3	95.8	6.8	0.1	0.4	4.8	0.3
PM-4	AGCGCGCCATAGAAGTGCGA	29.5	5.7	82.3	15.8	−0.5	0.4	5.0	0.9
PM-8	CGCGATGAACCGCTGTAGGCGG	28.4	4.1	78.5	11.6	−0.1	0.2	5.0	0.6
PM-6	AGCGATAACTCGCCCAGGCGG	33.1	2.7	91.5	7.7	−0.5	0.3	5.9	0.4
PM-1	TGCGATCGCACTTAGCGA	35.9	5.5	100.5	15.5	−1.3	0.3	6.0	0.9
PM-3	TGCGAGCCGTTGATAGCGG	35.8	3.6	98.8	9.7	−1.4	0.2	6.4	0.7
PM-9	GGCGAACTGGCGATATTAGCGG	39.2	3.9	109.5	11.1	−0.2	0.4	6.6	0.6
PM-5	AGCGAACTGGCGATTAGCGC	55.6	1.9	154.3	5.1	−1.3	0.2	9.6	0.4

between PM-2 × 2-N duplexes and the corresponding mismatched 2 × 2-N duplexes were found. The mean values of $\Delta\Delta G$ for these two duplex types were 2.1 ± 0.8 and 2.5 ± 1.1 kcal/mol, respectively. These average differences are depicted in Figure 4. Although a number of PM-N duplexes exhibited larger than average differences, a general sequence-dependent relationship with $\Delta\Delta G$ was not evident. Duplexes of each type are uniformly dispersed along the x-axes in Figures 2 and 3, implying no discernible sequence-dependent link with $\Delta\Delta G$ and ΔT_m. However, the data does suggest some dependence of $\Delta\Delta G$ values (Table 6 and Figure 4) on the type of duplex (i.e., PM, 2 × 2, and 4 × 4).

Discussion

Results of DNA melting experiments conducted on 53 short duplex DNAs, ranging in length from 18 to 22 base pairs, showed that specific buffer type can significantly influence the melting thermodynamics of short duplex DNA. For several reasons, this observation is both counter-intuitive and contrary to popular belief. According to the measured values, ΔG_{25} and T_m of all the short DNA duplexes are slightly more stable in NaCl/phosphate than in NaCl/cacodylate buffer, even though the total ionic strength is slightly lower (by 10.4 mM) in the NaCl/phosphate solvent. A simple argument based on electrostatics of charge neutralization is likely not the correct explana-

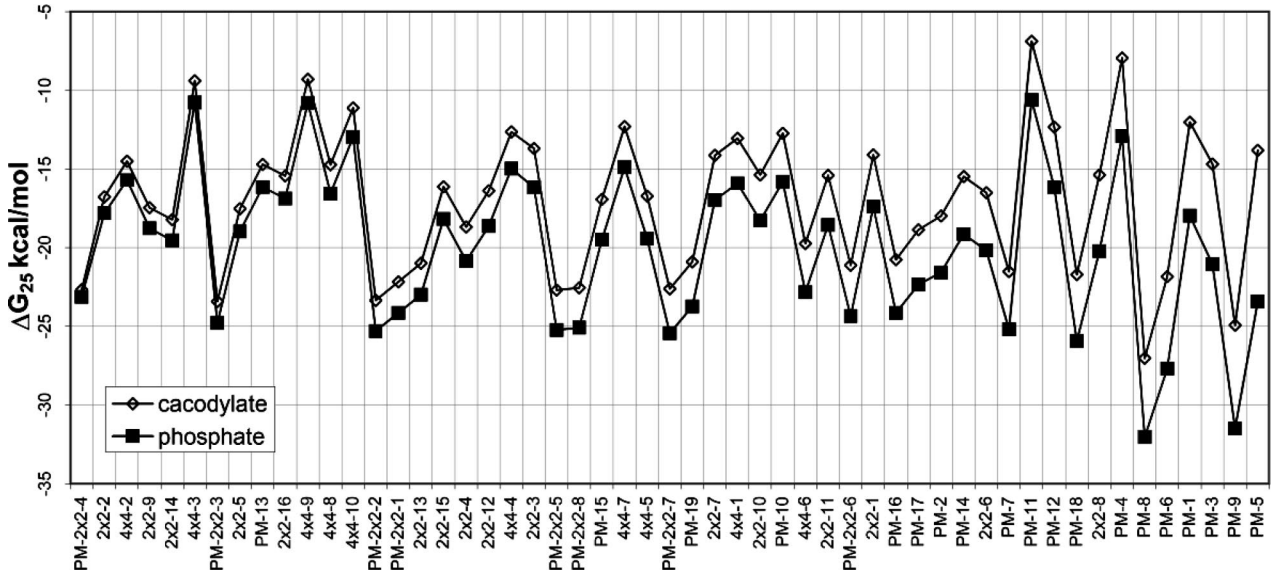

Figure 2. The free energy values for each duplex, measured in both buffers, sorted (left to right) from the least difference in free energy to the greatest difference.

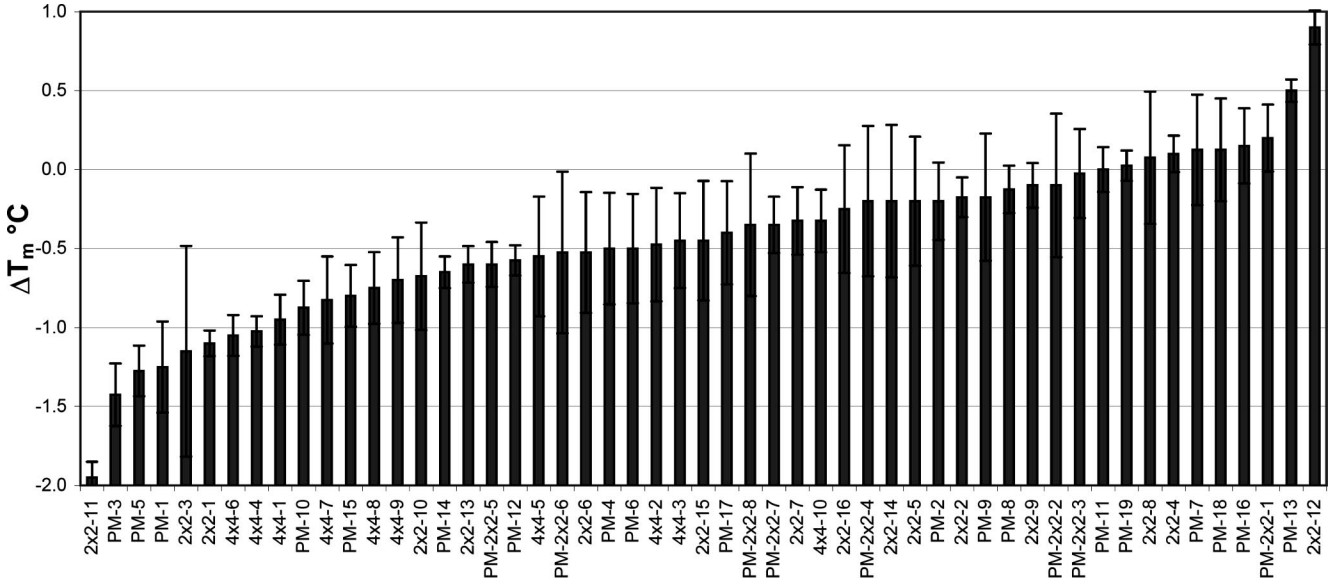

Figure 3. Difference in T_m values, T_m(cacodylate) − T_m(phosphate), for each duplex sorted from smallest difference (left) to greatest difference (right). Differences in melting temperature were found to vary from −2.0 ± 0.1 to 0.9 ± 0.1 °C with a mean difference of −0.4 ± 0.5 °C.

TABLE 6: The Average Differences between Cacodylate and Phosphate (from Table 5) Grouped by Duplex Type

	AVG $\Delta\Delta H$ kcal/mol	σ^2	AVG $\Delta\Delta S$ e.u.	σ^2	AVG ΔT_m °C	σ^2	AVG $\Delta\Delta G_{25}$ kcal/mol	σ^2
PM	23.3	10.9	65.6	30.1	−0.4	0.5	3.7	1.9
2 × 2 MM	16.1	7.1	46.2	20.6	−0.4	0.6	2.4	1.0
4 × 4 MM	16.5	4.6	48.4	13.4	−0.7	0.3	2.1	0.7
ALL	19.9	9.5	56.5	26.4	−0.4	0.5	3.0	1.7

tion for these observations. Alternatively, nonelectrostatic solvent effects on DNA sequence dependent hybridization and stability provide a more attractive explanation as follows.

Stability differences attributed to buffer identity observed here are reminiscent of the well-known Hofmeister series for protein stability.[26] Effects of Hofmeister ions on the stability of proteins have been analyzed through model compound studies that collectively indicate that the mechanism of action can be described by the weak interaction model.[26] Interactions specific to each ion are characterized by a salting-out or salting-in parameter that serves to rank the chemical species into a series relative to one another. Hofmeister ions are thought to influence overall protein stability by altering hydrogen-bonding properties of water, including those in the vicinity of the structure.

With this in mind, a viable explanation of the buffer-specific stabilities might be that different buffer environments induce differences in DNA hydration levels. Closer inspection of the two buffer species provides a plausible explanation of how DNA stability could be differentially affected by buffer identity. Arsenic lies below phosphorus on the periodic table and oxygen is to the right of carbon. Thus, cacodylate functional attachments are larger and bulkier than the oxygens attached to phosphate, while the phosphate ions having a central phosphorus atom are slightly smaller compared to the cacodylate ions. For buffers

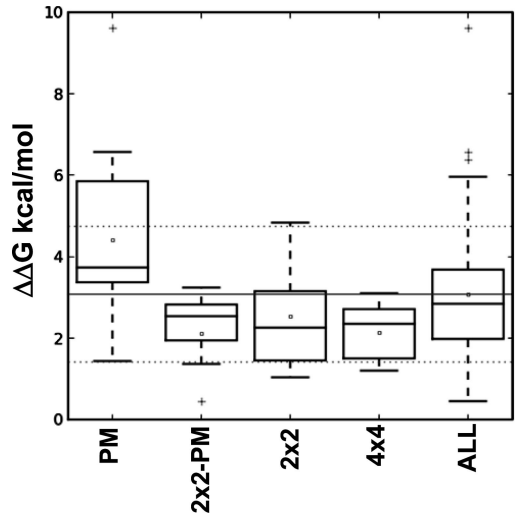

Figure 4. Summary of $\Delta\Delta G$ differences for all classes of DNA duplex molecules.

containing the larger cacodylate ions, steric differences exclude water from the hydration layer around the DNA and so act to dehydrate and destabilize the duplex. If one assumes that the DNA hydration volume is the same in both buffers, then more water will be excluded from DNA in cacodylate, resulting in greater dehydration and reduced stability. The smaller (phosphate) ions are more hydrated and will be more hydrophilic. As a result, more water molecules will be in the vicinity of the DNA, resulting in increased stability. A systematic and significant difference was seen for $\Delta H°$, $\Delta S°$, and $\Delta G°$ evaluated in the two melting buffers. Differences in T_m were smaller but still significant. For all thermodynamic parameters, the stability ordering was preserved in both buffers. No definitive correlation was found between sequence identity, length, %GC and the differences associated with different buffers. These observations are also consistent with a relative hydration effect that would not be expected to be strongly sequence dependent. It may be possible to further explore the role of water activity in relation to the observed buffer phenomena through studies of the influences of osmolytes in addition to buffer on the melting behavior of short duplex DNAs. Such investigations might provide additional support for the aforementioned geometric interpretation, but are beyond the scope of this study.

Another general, but more subtle observation was that stability differences in the two buffers were smaller for DNA duplexes containing mismatch regions. This suggests that the perturbed structure in mismatch duplex complexes may play a role. Ions exhibiting weaker interactions with water than water itself are known as structure-breakers or chaotropes, whereas ions that exhibit strong interactions with water molecules are referred to as structure makers or kosmotropes. Anions generally hydrate more strongly than cations with the same ionic radius because the hydrogen atoms in water can more closely approach the duplex than oxygen atoms of water (by about 0.8 Å). Furthermore, anions are more polarizable than cations. Since small ions are more strongly hydrated, they are more hydrophilic. Phosphate has a smaller ionic radius than cacodylate, thus is higher in the Hofmeister series (i.e., more chaotropic). Hofmeister effects become important at moderate to high salt concentrations (0.01−1.0 M), corresponding to average interionic distances of 4.4−0.94 nm, although where higher sensitivity can be attained, the lower limit is pushed downward.[26,27] At the high salt concentrations needed to observe the anion effect, there are only minor differences in the T_m values when the cations are Li^+, Na^+, or K^+. Increasing the sodium ion concentration would likely amplify the differences observed in thermodynamic parameters evaluated in the two buffers.[28,29] There is a greater degree of exposure of the bases to solvent in the denatured state of DNA than in the native duplex form; and there surely is also a larger degree of exposure of mismatch bases within duplex molecules.[30]

The potential consequences of $\Delta\Delta G_{25} \approx 3$ kcal/mol for phosphate versus cacodylate buffer on the reaction equilibrium constant are sizable. Because of the exponential nature of the equilibrium constants for DNA hybridization, relatively small errors in the measurement of free-energy propagate to significantly larger errors in the calculation of equilibrium constants. If an error of ε is encountered in the measurement of ΔG, i.e. $\Delta G_2 = \Delta G_1 + \varepsilon$, this error manifests itself in the equilibrium constant written as, $K_2 = e^{(-\Delta G_2/RT)} = e^{(-\Delta G_1 - \varepsilon/RT)} = K_1 \cdot e^{(-\varepsilon/RT)}$. For example, an error of $\varepsilon = 3$ kcal/mol results in a factor of 158 in the equilibrium constant (at $T = 298.15$ K). When explicitly represented as such, this somewhat small effect can have a significant impact on predicted hybridization propensities in multiplex reaction schema. Although errors apply uniformly to all reacting species in the reaction (i.e., perfect match duplexes or cross-hybrids), quantitative and accurate predictions of hybridization behavior requires explicit knowledge of the sources of thermodynamic stability.[10]

Conclusions

DSC melting studies of 53 short DNA duplexes in ~1.0 M Na^+ solvent containing either sodium cacodylate or sodium phosphate buffer revealed statistically significant differences in stability associated with the different buffer species. Higher stability was observed in the NaCl/phosphate than in the NaCl/cacodylate buffer. The observed stability differences are independent of sequence identity but are more pronounced for duplexes having the least perturbed duplex structure (i.e., perfect match duplexes). Results are consistent with relative locations of the buffer anions in the Hofmeister series and how they may differentially affect local hydration levels surrounding the DNA duplex. The disparity in stability for the two buffers reveals that thermodynamic parameters evaluated from DNA melting experiments are not independent of the buffer species. Therefore, in predictive methods for design and optimization of reliable DNA hybridization results, in addition to [Na^+], buffer identities should also be carefully considered.

Supporting Information Available: This material is available free of charge via the Internet at http://pubs.acs.org.

References and Notes

(1) SantaLucia, J., Jr. A unified view of polymer, dumbbell, and oligonucleotide DNA nearest-neighbor thermodynamics. *Proc. Natl. Acad. Sci. U.S.A.* **1998**, *95* (4), 1460–5.

(2) SantaLucia, J., Jr.; Allawi, H. T.; Seneviratne, P. A. Improved nearest-neighbor parameters for predicting DNA duplex stability. *Biochemistry* **1996**, *35* (11), 3555–62.

(3) SantaLucia, J., Jr.; Hicks, D. The thermodynamics of DNA structural motifs. *Annu. Rev. Biophys. Biomol. Struct.* **2004**, *33*, 415–40.

(4) Allawi, H. T.; SantaLucia, J., Jr. Nearest-neighbor thermodynamics of internal A.C mismatches in DNA, Sequence dependence and pH effects. *Biochemistry* **1998**, *37* (26), 9435–44.

(5) Allawi, H. T.; SantaLucia, J., Jr. Nearest neighbor thermodynamic parameters for internal G.A mismatches in DNA. *Biochemistry* **1998**, *37* (8), 2170–9.

(6) Allawi, H. T.; SantaLucia, J., Jr. Thermodynamics of internal C.T mismatches in DNA. *Nucleic Acids Res.* **1998**, *26* (11), 2694–701.

(7) Allawi, H. T.; SantaLucia, J., Jr. Thermodynamics and NMR of internal G.T mismatches in DNA. *Biochemistry* **1997**, *36* (34), 10581–94.

(8) Dawson, R. M. C.; Elliott, D. C.; Elliott, W. H.; Jones, K. M. *Data for biochemical research*; Clarendon Press: Oxford, 1986.

(9) Fasman, G. D. *Practical handbook of biochemistry and molecular biology*; CRC Press: Boca Raton, FL, 1989.

(10) Horne, M. T.; Fish, D. J.; Benight, A. S. Statistical thermodynamics and kinetics of DNA multiplex hybridization reactions. *Biophys. J.* **2006**, *91* (11), 4133–53.

(11) Ruzin, S. E. *Plant microtechnique and microscopy*: Oxford University Press: New York, 1999.

(12) Good, N. E.; Winget, G. D.; Winter, W.; Connolly, T. N.; Izawa, S.; Singh, R. M. M. Hydrogen ion buffers for biological research. *Biochemistry* **1966**, *5*, 467–477.

(13) Chalikian, T. V.; Völker, J.; Plum, G. E.; Breslauer, K. J. A more unified picture for the thermodynamics of nucleic acid duplex melting: A characterization by calorimetric and volumetric techniques. *Proc. Natl. Acad. Sci. U.S.A.* **1999**, *96*, 7853–7858.

(14) Jelesarov, I.; Crane-Robinson, C.; Privalov, P. L. The energetics of HMG box interactions with DNA: thermodynamic description of the target DNA duplexes. *J. Mol. Biol.* **1999**, *294* (4), 981–995.

(15) Privalov, P. L.; Jelesarov, I.; Read, C. M.; Dragan, A. I.; Crane-Robinson, C. J. The energetics of HMG box interactions with DNA: thermodynamics of the DNA binding of the HMG box from mouse sox-5. *J. Mol. Biol.* **1999**, *294* (4), 997–1013.

(16) Holbrook, J. A.; Capp, M. W.; Saecker, R. M.; Record, M. T., Jr. Enthalpy and heat capacity changes for formation of an oligomeric DNA duplex: interpretation in terms of coupled processes of formation and association of single-stranded helices. *Biochemistry.* **1999**, *38* (26), 8409–8422.

(17) Riccelli, P. V.; Vallone, P. M.; Kashin, I; Faldasz, B. D.; Lane, M. J.; Benight, A. S. Thermodynamic, spectroscopic, and equilibrium binding studies of DNA sequence context effects in six 22-base pair deoxyoligonucleotides. *Biochemistry* **1999**, *38* (34), 11197–208.

(18) Vallone, P. M.; Benight, A. S. Thermodynamic, spectroscopic, and equilibrium binding studies of DNA sequence context effects in four 40 base pair deoxyoligonucleotides. *Biochemistry* **2000**, *39* (26), 7835–46.

(19) Bevington, P. R. *Data reductions and error analysis for the physical sciences*; McGraw-Hill: NY, 1969.

(20) Chou, S. H.; Chin, K. H. Solution structure of a DNA double helix incorporating four consecutive non-Watson−Crick base-pairs. *J. Mol. Biol.* **2001**, *312* (4), 769–81.

(21) Chou, S. H; Zhu, L.; Reid, B. R. On the relative ability of centromeric GNA triplets to form hairpins versus self-paired duplexes. *J. Mol. Biol.* **1996**, *259* (3), 445–57.

(22) Chou, S. H.; Chin, K. H.; Wang, A. H. Unusual DNA duplex and hairpin motifs. *Nucleic Acids Res.* **2003**, *31* (10), 2461–74.

(23) Chou, S. H.; Chin, K. H. Quadruple intercalated G-6 stack, A possible motif in the fold-back structure of the drosophila centromeric dodeca-satellite. *J. Mol. Biol.* **2001**, *314* (1), 139–52.

(24) Greene, K. L.; Jones, R. L.; Li, Y.; Robinson, H.; Wang, A. H.; Zon, G.; Wilson, W. D. Solution structure of a GA mismatch DNA sequence, d(CCATGAATGG)2, determined by 2D NMR and structural refinement methods. *Biochemistry* **1994**, *33* (5), 1053–62.

(25) Cheng, J. W.; Chou, S. H.; Reid, B. R. Base pairing geometry in GA mismatches depends entirely on the neighboring sequence. *J. Mol. Biol.* **1992**, *228* (4), 1037–41.

(26) Cacace, M. G. ; Landau, E. ; M, Ramsden, J. J. The Hofmeister series, Salt and solvent effects on interfacial phenomena. *Q. Rev. Biophys.* **1997**, *30* (3), 241–77.

(27) Collins, K. D.; Washabaugh, M. W. The Hofmeister effect and the behaviour of water at interfaces. *Q. Rev. Biophys.* **1985**, *18* (4), 323–422.

(28) Hamaguchi, K.; Geiduschek, E. P. The effect of electrolytes on the stability of the deoxyribonucleate helix. *J. Am. Chem. Soc.* **1962**, *84*, 1329–1338.

(29) Lavelle, L.; Fresco, J. R. Stabilization of nucleic acid triplexes by high concentrations of sodium and ammonium salts follows the Hofmeister series. *Biophys. Chem.* **2003**, *105*, 681–699.

(30) Robinson, D. R.; Grant, M. E. The effects of aqueous salt solutions on the activity coefficients of purine and pyrimidine bases and their relation to the denaturation of deoxyribonucleic acid by salts. *J. Biol. Chem.* **1966**, *241*, 4030–4042.

JP809310W